ACCELERATOR PHYSICS CHALLENGES FOR THE NSLS-II PROJECT*

S. Krinsky# for NSLS-II Design Team

NSLS-II, BNL, Upton, New York, 11973-5000, U.S.A.

Abstract

The NSLS-II is an ultra-bright synchrotron light source based upon a 3-GeV storage ring with a 30-cell (15 super-period) double-bend-achromat lattice with damping wigglers used to lower the emittance below 1 nm. In this paper, we discuss the accelerator physics challenges for the design including: optimization of dynamic aperture; estimation of Touschek lifetime; achievement of required orbit stability; and analysis of ring impedance and collective effects.

INTRODUCTION

The NSLS-II storage ring [1-5] is a 30-cell (15-superperiod) double-bend achromat structure (with 30 zero-dispersion straights): 15 low-betax (short) straights of length 6.6m and 15 high-betax (long) straights of length 9.3m (see Figure1).   One long straight is used for injection and two are used for RF cavities.   In the baseline design, three long straights are used for damping wigglers (1.8T peak field, 7-m length) which lower the horizontal emittance down from 2nm-rad to 1nm-rad. As the ring is built out, additional damping wigglers and the user insertion devices can lower the emittance to ~0.5nm-rad. In- vacuum undulators with full-gaps as small as 5mm will provide very high brightness x-ray sources. Elliptically polarized devices will also provide important sources for user research. Some of the key project goals are listed in Table 1.

The dipole magnets have the relatively low field of 0.4T in order to make the damping wigglers more effective in reducing the emittance. In order to provide hard x-ray dipole-like sources, three-pole wigglers with 1T peak field will be placed just upstream of the downstream dipoles in the achromatic bends. Of the 60 dipoles, 54 have a magnet gap of 35mm and 6 have a larger gap of 90 mm in order to facilitate extraction of far infrared radiation.

Table 1: Project Goals

Beam Property	Goal
Horizontal emittance (nm-rad)	1
Vertical emittance (nm-rad)	0.010
Average current (mA)	500
Straights for insertion devices	27
Three pole wigglers	15-30
Orbit stability (% of beam size)	10
Touschek lifetime (hrs)	>3
Top-off injection frequency (/min)	<1

The 500MHz RF system provides 1320 buckets and the design average current is 500mA with ~1000 bunches. Third-harmonic RF cavities will be used to lengthen the bunches from ~15ps to ~30ps assuring a Touschek lifetime >3hrs.   Operation will be based on top-off injection.

LATTICE

The lattice as described in the NSLS-II Preliminary Design Report [1] has quadrupole triplets bounding the insertions. Two sextupoles/cell in the dispersive region are used to correct the chromaticity and 7 geometric sextupoles/cell (4 bounding the long straight and 3 bounding the short straight) are used to reduce the tune-shift with amplitude and critical resonance terms. Tracking studies show good dynamic aperture.
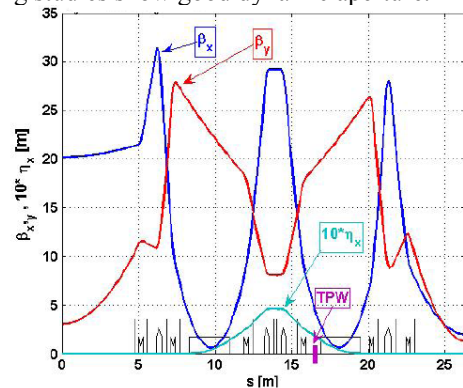

Figure 1: One cell of NSLS-II lattice from Preliminary Design Report [1]. A super-period consists of this cell plus its reflection about either insertion center. The long high-betax straight is on the left and the short low-betax insertion is on the right.

Recent work [6,7] has focused on the inclusion of the damping wigglers. Care has been necessary in matching the linear optics after inclusion of the damping wigglers. One good approach has been to use the three bounding quadrupoles to maintain $\alpha_x=\alpha_y=0$ at the insertion center as well as to hold fixed the horizontal phase advance. The vertical betafunction is not restricted but is found to exhibit only small variation.

It has been found that three sextupoles bounding the long straight are sufficient rather than the four in the preliminary design.   It has also been shown that the momentum aperture can be increased by providing a third chromatic sextupole knob in the dispersion region between the two dipoles in each cell. Two approaches have been analyzed: (1) replacement of a dipole corrector by a combination sextupole/dipole corrector [6]; (2) movement of one of the existing defocusing sextupoles in the dispersion region in each cell towards the focusing sextupole at the dispersion maximum [7].

Inclusion of the additional chromatic sextupole knob allows one to reduce the second-order chromaticity while maintaining flexibility in the geometric sextupoles to correct the tune-shift with amplitude. Results from the first approach [6] are shown in Figures 2-4. Analysis of the benefits of adding a third chromatic knob is on-going.
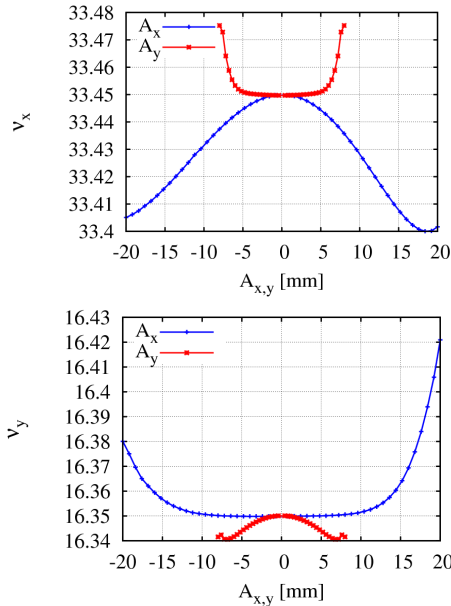

Figure 2: Dependence of horizontal (top) and vertical (bottom) tune on amplitude.
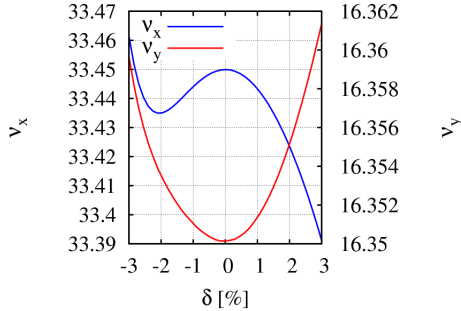

Figure 3: Dependence of horizontal (blue) and vertical (red) tune on energy.
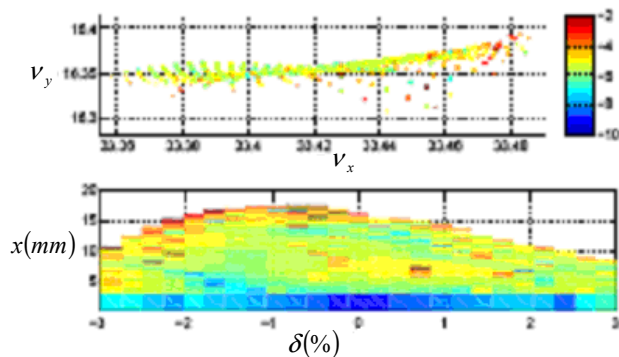

Figure 4: Frequency map: momentum deviation-horizontal in midplane (y~0) including errors.

TOUSCHEK LIFETIME

Since a primary goal of the NSLS-II design is to achieve small transverse emittance and hence small transverse bunch dimensions, intrabeam scattering is a fundamental concern. Multiple intrabeam scattering can increase the emittance but it has been shown that this is a small effect for NSLS-II [8] (see Figure 5). Lowering the emittance by increasing the amount of damping wiggler radiation does not result in large IBS-induced emittance blow-up since higher beam density is compensated by faster radiation damping. Single intrabeam (Touschek) scattering leads to reduced lifetime. At NSLS-II we require the Touschek lifetime to be maintained above 3 hrs. in order to keep the time between top-off injections greater than 1 min.

Large Touschek lifetime requires sufficient momentum aperture. Assuming the RF voltage is set to provide a longitudinal bucket with 3% energy acceptance, the major concern is that nonlinear transverse dynamics can reduce the energy acceptance below acceptable levels. Simple considerations allow one to determine the requirements on the momentum aperture [9].

In the regions of high dispersion, scattered electrons which experience energy deviation undergo a tune deviation and find themselves oscillating about a displaced closed orbit. This displacement leads to large betatron amplitude which may exceed the dynamic aperture. In these high dispersion regions it is very challenging to achieve large energy acceptance. Fortunately, for large dispersion, the horizontal beam size is big so the scattering rate is low.
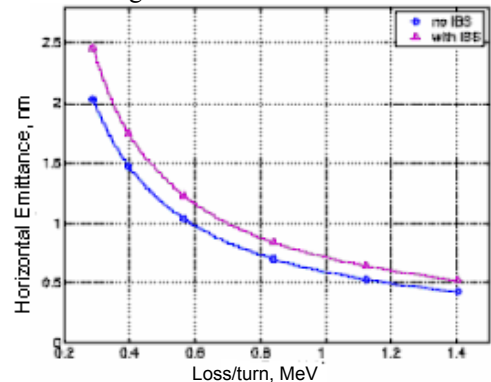

Figure 5: Horizontal emittance vs. total radiation loss.

In regions of zero dispersion, the horizontal beam size is small so the scattering rate is high. However, scattered electrons find themselves only slightly displaced from the new closed orbit (due to higher-order dispersion), so it is not as difficult to achieve large energy acceptance. For this reason the requirement on energy acceptance can be loosened in the high dispersion regions. In Table 2, we illustrate the dependence of the Touschek lifetime on the energy acceptance (δ_{acc}) in the high and low dispersion regions. The lifetimes are estimated from Bruck's formula [9] for a 15ps bunch without Landau cavity. The lifetime with Landau cavity would be twice as long.

Table 2: Touschek lifetime

δ_{acc} (η small)	δ_{acc}(η large)	Lifetime (hrs)
3%	2.5%	5.5
2.5%	2.5%	3.3
2.5%	2.0%	2.9
2.5%	1.5%	2.3

It is seen that achievement of an energy acceptance of 2.5% in the zero dispersion straights and 2.0% in the high dispersion regions would provide a 5.8 hr Touschek lifetime with Landau cavity which exceeds our minimum requirement. Tracking studies show that this can be achieved when the linear chromaticity is corrected to small positive values.   Current work is aimed at determining what energy acceptance can be achieve when the linear chromaticity is corrected to larger values (~5) desired to provide head-tail damping.

HIGHER-ORDER MULTIPOLE ERRORS

If an electron traveling along the ideal closed orbit Touschek scatters and undergoes a momentum deviation $\delta = \Delta p / p$ at a position with dispersion $\eta = \eta_1 + \eta_2 \delta$, then it suddenly finds itself displaced from its new closed orbit by $\eta \delta$. If it returns to this point with a betatron phase change of 180°, then it will be displaced from the ideal orbit by $2\eta\delta$. For NSLS-II, including the effects of nonlinear dispersion, an electron which gains 2.5% of its energy will experience a displacement of 20mm from the ideal orbit at the dispersion maximum, while an electron which loses 2.5% of its energy will experience a larger displacement of 28mm [9,10] (see Figure 6). As a consequence, higher-order multipole errors have a greater influence on the dynamic aperture for negative δ.
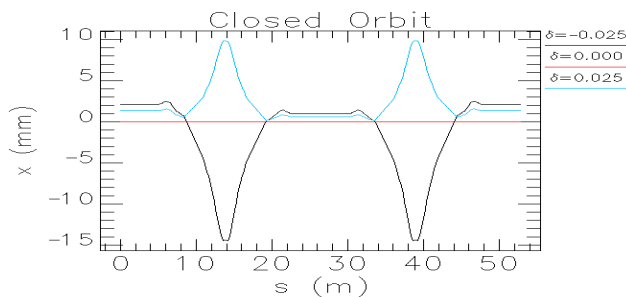

Figure 6:   The off-momentum closed orbit for energy deviations of δ=+/-2.5%.   Note that the nonlinear dispersion increases the orbit deviation for negative δ.

Analysis showed [10] that in order to keep particles displaced by as much as 28mm it was necessary to set a tight tolerance on the higher-order multipoles in the quadrupoles and sextupoles located near the maximum dispersion.   This was achieved by designing these particular magnets with a larger aperture.   The

quadrupoles at large dispersion have a radius of 90mm while the regular quadrupoles have a radius of 66mm. The sextupoles at the large dispersion have a radius of 76mm while the regular sextupoles have a radius of 68mm. In Table 3, we present the systematic higher-order multipole tolerances for the quadrupoles and sextupoles. The quantity B_n is the contribution of the n-th multipole to the magnetic field at a radius of R=25mm, divided by the ideal quadrupole or sextupole field at this radius. One unit represents a fractional contribution of one part in 10^4. Random higher-order multipole errors are also found to be important and must be controlled by careful construction of the magnets.

Table 3: Systematic Multipole Tolerances (R=25mm)

	n	$B_n(10^{-4})$ regular	$B_n(10^{-4})$ large aperture
Quad	6	1.0	1.0
Quad	10	4.5	0.5
Quad	14	4.0	0.1
Sext	9	1.0	0.5
Sext	15	1.0	0.5
Sext	21	4.0	0.5

INJECTION

Top-off injection is a fundamental aspect of the NSLS-II design. In order to meet user requirements, we will restrict the frequency of top-off injections to be less than once per minute. Maintaining a Touschek lifetime greater than 3 hours will limit the required charge in an injected bunch train to less than 8nC. The injector system design is sufficiently flexible to allow hunt and peck injection to limit charge variation per bunch. The baseline design of the storage ring injection straight uses four carefully matched pulsed kicker magnets to bring the orbit close to the septum for injection. In order to minimize disturbance of the stored beam during the injection process, it is necessary to meet extremely tight tolerances on matching the kicker waveforms and on their reproducibility. For this reason, we are studying [11] an alternate approach introduced at KEK [12] which uses a single pulsed sextupole magnet. The advantage of this method is that since the stored beam passes through the center of the sextupole where the field is minimal, disturbance to the stored beam can be made very small. Also, this approach uses only one fast pulsed magnet avoiding the difficulty of matching waveforms for different magnets. On the other hand using the pulsed sextupole presents its own challenges: the injected beam which passes through the sextupole off-center experiences a large quadrupole gradient in addition to the desired dipole kick. Also, to minimize the disturbance to the stored beam, it is necessary to satisfy a very stringent tolerance on the position of the stored beam in the sextupole.

Top-off safety analysis [13] is being pursued. We are using software developed recently at SSRL/SLAC [14]

and ALS/LBL [15]. It is our goal to identify required apertures and interlocks early in the design so that we can most efficiently assure that no injected electrons can travel down a user beamline. Based on the experience at other facilities, we are working to identify error scenarios and carry out tracking studies to assure the design is safe.

MAGNET TOLERANCES

An important aspect of the NSLS-II design is the accurate placement of the quadrupoles and sextupoles on girders. Using the vibrating wire technique [16,17], the multipole centers will be placed on a straight line to $30\,\mu m$ tolerance. Girders will be placed relative to one another within a $100\,\mu m$ tolerance. Beam based alignment [18] will be used to calibrate the RF beam position monitors relative to the quadrupole centers to within $30\,\mu m$.

Dipole, quadrupole and sextupole power supply stability requirements are within standard achievable limits , <25ppm for dipoles and <50ppm for multipoles, where the tolerance is for full peak-to-peak variation.

Great care has been taken in the conventional facility design to isolate the concrete floor from roof supports and from vibrating mechanical equipment. The goal is to keep vertical floor motion below 25nm in the frequency bandwidth 4-50 Hz, where the motion is expected to be uncorrelated. The magnets will be placed on specially designed girders [19] which have no resonance below 50 Hz, so there will be negligible amplification of vibration amplitude from the floor to the top of the girder for frequency below 50 Hz. Floor motion falls off fast at higher frequency, see Figure 7. Therefore, even if there is some amplification by the girder above 50 Hz, the effect on the electron beam will be small. The floor motion at frequencies below 4 Hz can be significantly larger. The effect on the electron beam of vibrations with frequency below 4 Hz is reduced since the associated wavelength is long and major portions of the storage ring containing many girders move together. However, we can expect significant motion of the electron beam with frequency below 4 Hz that will need to be reduced by feedback.
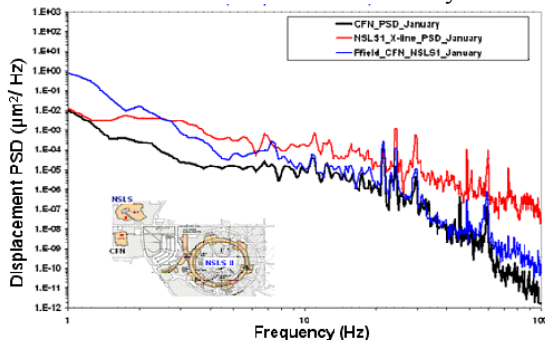

Figure 7: Vertical power spectrum density measured [20] at the NSLS-II site in January 2007.

ORBIT STABILITY

The electron beam at the center of the short straight has an rms vertical beam size of $3\,\mu m$. Therefore, the orbit motion must be held below $0.3\,\mu m$ at this location. This is a very challenging goal and our strategy to accomplish this, as well as hold the orbit stable at all other sources, is based on optimization of a global orbit feedback system. Special RF beam position monitors (BPMs) on thermally stable stands will be placed at each end of the undulators in the short straights. In addition, there will be six BPMs per cell mounted on the vacuum chamber. Orbit alignment will be carried out using six slow correctors per cell with maximum strength of 0.8 mrad. Fast orbit feedback [21] will be implemented using 3 fast correctors per cell with maximum strength of $20\,\mu rad$ (see Figure 8).
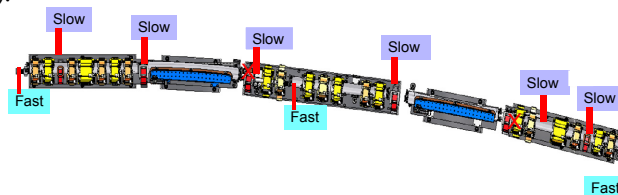

Figure 8: The locations of 6 slow correctors and 3 fast correctors per cell.

In order to limit the noise caused by digital step changes of the power supplies in the feedback system, the angular kick corresponding to the last bit of the power supplies for the fast correctors must be smaller than 3 nrad. Designing the system with strong slow correctors and weak fast correctors avoids the requirement of building power supplies with large strength and small step size. Initial operation of the orbit feedback system will use only input from the RF BPMs but the system will be designed to allow for later incorporation of input from x-ray BPMs.

COLLECTIVE EFFECTS

The goal is for NSLS-II to run with 500mA, with ~1000 bunches each contributing ~0.5mA. There will be four (or more) ion-clearing gaps in the bunch pattern to reduce the growth rate of the fast-ion instability [22]. Estimates on the electron cloud [23] indicate it should not pose a problem. Using top-off injection the total current will be maintained constant to within 1% and individual bunch currents will be kept within a range of about 20%. Passive third-harmonic Landau cavities [1] will be used to double the average bunch length from 15 to 30ps. Higher-order modes in the superconducting RF cavities will be sufficiently damped to avoid coupled bunch instabilities. We do not expect there to be longitudinal coupled bunch instability. The threshold for the longitudinal microwave instability is estimated to be above 5mA per bunch. The resistive wall impedance and the fast-ion instability can drive coupled bunch vertical instability. Transverse bunch-by-bunch digital feedback is included in the NSLS-II baseline design. In addition, if

sufficient dynamic aperture can be achieved with positive vertical chromaticity of ~4 or 5, this would stabilize the transverse motion [24].

There has been an on-going effort to compute the wakefields generated by all of the storage ring components [1, 25-27] using the 3-D electromagnetic simulation program GdfidL [28]. Our approach is two-fold: (1) We first compute the wakefields generated by a charge distribution of 3-mm length; (2) Next we compute the wakefield due to a much shorter charge distribution to be used as a pseudo-Greens function [29] in a particle tracking code TRANFT [30].

In Figure 9, we summarize the relative contribution of the components of the storage ring to the loss factor of a 3-mm charge distribution. We see that the dominant contributions are from the resistive wall impedance and the tapers for the RF cavity transitions. In Figure 10, we summarize the relative contributions of the components of the storage ring to the vertical kick factor for a charge distribution length $\sigma_s = 3mm$. The dominant contribution comes from the resistive wall and geometric impedance of the in-vacuum undulators (IVUs).
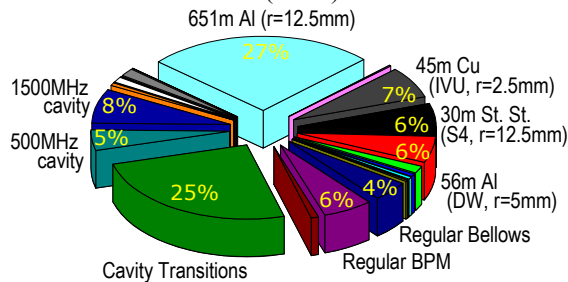

Figure 9: Contribution of the individual components and resistive wall effect to the total longitudinal impedance in terms of the loss factor for $\sigma_s = 3mm$.
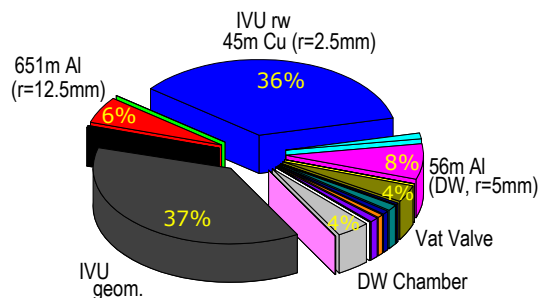

Figure 10: Contribution of the individual components and resistive wall effect to the total vertical dipole impedance in terms of the vertical kick factor for $\sigma_s = 3mm$.

CONCLUDING REMARKS

The accelerator physics design of NSLS-II is now mature and provides a firm basis for the achievement of the project goals.

ACKNOWLEDGEMENTS

The work reported in this paper is due to the work of many individuals and I wish to thank all of them for their enthusiastic efforts to elucidate the accelerator physics issues for NSLS-II. Special thanks are due to Ferdinand Willeke and Satoshi Ozaki for their support.

REFERENCES

[1] NSLS-II Preliminary Design Report, http://www.bnl.gov/nsls2/project/PDR/.
[2] S. Krinsky, J. Bengtsson, and S.L. Kramer, Proc. EPAC06, p3487.
[3] S. Ozaki, J. Bengtsson, S.L. Kramer, S. Krinsky, V.N. Litvinenko, Proc. PAC07, p77.
[4] S.L Kramer, J. Bengtsson, S. Krinsky, V.N. Litvinenko, and S. Ozaki, Proc. APAC07, p613.
[5] J. Bengtsson, Proc. EPAC08, p988.
[6] J. Bengtsson, "NSLS-II : Control of Dynamic Aperture," BNL-81770-2008-IR.
[7] W. Guo, "New Approach in Lattice Design and Optimization with Insertion Devices," Proc. PAC09.
[8] B. Podobedov, Proc. PAC07, p1353.
[9] B. Nash, Touschek Lifetime Calculations for NSLS-II, Proc. PAC09.
[10] B. Nash and W. Guo, "Impact of Higher-Order Multipole Errors on Dynamic and Momentum Aperture," Proc.PAC09.
[11] H. Takaki et al., Proc. EPAC08, p2204.
[12] T. Shaftan et al., "Alternative Designs of the NSLS-II Injection Straight Section," Proc. PAC09.
[13] Y. Li et al., "Top-Off Safety Analysis for NSLS-II," Proc. PAC09.
[14] A. Terebilo, private communication.
[15] H. Nishimura et al., Proc. PAC07, p1173.
[16] A. Jain, et al, International Workshop on Accelerator Alignment, Tsukuba, Japan, Feb.11-15, 2008. http://www.slac.stanford.edu/econf/C0802113/
[17] S.L. Kramer and A. Jain, "Specifications and R&D Program on Magnet Alignment Tolerances for NSLS-II," Proc. PAC09.
[18] L.H. Yu, "Beam Based Alignment and BPM Calibration," unpublished.
[19] S. Sharma, in NSLS-II Preliminary Design Report.
[20] N. Simos, M. Fallier and H. Amick, Proc. EPAC08, p181.
[21] L.H. Yu et al., Proc. EPAC08, p3315; I. Pinayev, Proc. EPAC08.
[22] G. Stupakov and L. Wang, "Fast-Ion Instability in NSLS-II," unpublished.
[23] L. Wang, "Study of Electron Cloud in NSLS-II," unpublished.
[24] S. Krinsky et al., Proc. PAC07, p1344.
[25] A. Blednykh and S. Krinsky, Proc. PAC07, p4321.
[26] A. Blednykh, "Infrared Extraction Chamber for NSLS-II," Proc. PAC09.
[27] A. Blednykh, "Impedance Calculations for the NSLS-II Storage Ring," Proc. PAC09.
[28] W. Bruns, GdfidL, http://www.gdfidl.de.
[29] A. Blednykh et al., "Microwave Instability Simulations for NSLS-II," Proc. PAC09.
[30] M. Blaskiewicz, "The TRANFT User's Manual version 1.0", BNL-77074-2006-IR, 2006.